

Observing and Modeling Ultracompact Binaries Detectable by LISA

OLIVIA COOPER,¹ MENTORS: MICHAEL W. COUGHLIN,² SHREYA ANAND,² AND MICHAEL L. KATZ³

¹*Department of Astronomy, Smith College, Northampton, MA 01063, USA*

²*Division of Physics, Math, and Astronomy, California Institute of Technology, Pasadena, CA 91125, USA*

³*Department of Physics and Astronomy, Northwestern University, Evanston, IL 60208, USA*

(Dated: September 28, 2019)

ABSTRACT

Our galaxy is rich with a menagerie of binary stellar remnants, many of which emit both gravitational and electromagnetic (EM) radiation as they rapidly orbit each other in ultracompact binary systems (UCBs). According to general relativity, UCBs strongly emit low frequency gravitational-waves (GW) detectable by the future Laser Interferometer Space Antenna (LISA). To predict and verify UCB GW detections and maximize LISA’s scientific potential, we observe a sample of UCB candidates using instruments including Palomar Observatory’s Triple Spectrograph and Kitt Peak’s Electron Multiplying CCD. With orbital periods on the order of minutes to hours, we observe multiple orbital phases or even full orbits, and measure orbital parameters such as radial velocity, mass, and inclination. We also generate a catalog, informed by Galactic binary population models, of gravitational waveforms and light curves for white dwarf UCBs in decaying orbits. These simulations constrain the range of binary parameters (including radial velocity, mass, and GW strain) that we expect to detect with time domain surveys such as the Zwicky Transient Facility and Large Synoptic Survey Telescope, which will contribute to the sample of LISA verification binaries.

1. INTRODUCTION

Massive objects causing a changing quadrupole moment in spacetime, such as the rapid decaying orbit and merger of dense stellar remnants, produce gravitational-waves (GW). While these ripples or waves are created by any and every source of gravity, the resulting change in spacetime curvature is negligible except for in extreme cases such as in the early Universe and near dense objects including black holes, neutron stars, and white dwarfs.

The Laser Interferometer Gravitational-wave Observatory (LIGO) has brought forth a new age of astrophysics by not only detecting a number of GW events—the coalescence of binary black holes (BBH) and neutron stars (BNS)—but also by realizing a new scientific domain, multi-messenger astrophysics. The inspiral and merger of light-emitting GW events such as BNS collisions, or kilonovae, provide the opportunity to observe these events in both the GW and electromagnetic (EM) regimes. With both GW and EM data, we can better constrain the binary system’s parameters such as location, masses, and inclination, as well as study host galaxy properties, r-process production constraints (Rosswog et al. 2018), equations of state of supranuclear density matter (Coughlin et al. 2018), and estimate the Hubble constant (Hotokezaka et al. 2018). Us-

ing these multi-messenger techniques, we can not only paint a fuller picture of the binary system, but can also use the system as an astronomical laboratory.

The scope of multi-messenger astrophysics and range of objects we can observe in both EM and GW domains will be broadened with the launch of future gravitational wave observatories like LISA, the Laser Interferometer Space Antenna (LISA Scientific Collaboration 2017). LISA is a space-based detector, currently proposed to launch in an Earth-trailing heliocentric orbit in 2034, which will have 3 test masses separated by 2.5 million km arms. Operating in a lower frequency band than LIGO, LISA sensitivity ranges from Hz to sub-Hz with peak sensitivity at about 5 mHz. LISA will be sensitive to very massive BBH, including some super-massive BBH in galaxy mergers, as well as resolvable Galactic binaries.

LISA sensitivity peaks at about 5 mHz, comparable to the expected frequency of a GW signal from Galactic binaries in ultracompact orbits (Burdge et al. 2019). Beyond the BNS and BBH detectable by LIGO, our galaxy is rich with a menagerie of binary objects. Many of these objects evolve into dense stellar remnants rapidly orbiting each other in ultracompact binary systems (UCBs). These binaries can be detached or interacting, and are characterized by periods of one hour

or shorter (Nelemans & van Haften 2013). UCBs provide insight into many poorly understood stellar processes including common-envelope evolution, magnetic braking, and massive star evolution (Nelemans & van Haften 2013). UCBs emit GWs strongly in the low frequency regime which the future space based GW detector, LISA, is highly sensitive to (Nelemans & van Haften 2013). LISA will detect slowly inspiraling binaries rather than only the compact binary coalescence events LIGO has detected thus far, and is predicted to detect $>27,000$ UCBs (Kupfer et al. 2018).

UCBs that emit strong GWs in the LISA band will be used to calibrate the signal we get from LISA. To verify and test future LISA detections, we can use optical data to identify and analyze UCBs in the electromagnetic (EM) regime. Figure 1 compares the LISA sensitivity derived from code¹ from Robson et al. (2019) to the predicted GW signals from a few notable UCBs. According to general relativity, UCBs like these systems emit significant gravitational radiation and will dominate GW signals in the mHz regime (Nissanke et al. 2012).

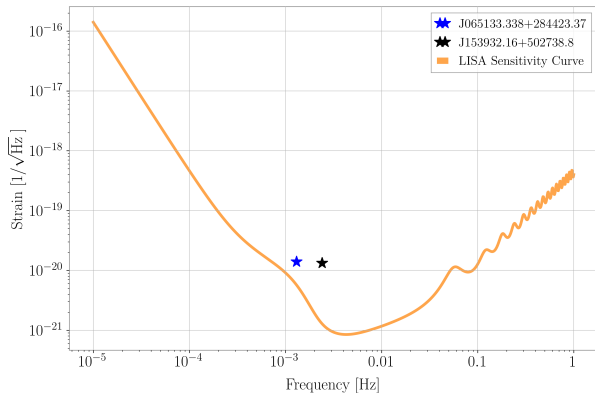


Figure 1. Amplitude spectral diagram for LISA showing the expected sensitivity (strain) of the detector at a given frequency. The blue and black points show estimated GW strain of two known UCBs, J065133.338+284423.37, a 12.75 minute period detached white dwarf binary (Hermes et al. 2012), and J153932.16+502738.8, a 6.91 minute binary that is the shortest period eclipsing binary system known (Burdge et al. 2019). Both objects have been studied with time-resolved photometry and spectroscopy and are detectable by LISA.

One type of UCB, double white dwarfs (DWDs) are very common in our Galaxy as over 97% of stars evolve

into white dwarfs (Korol et al. 2017). We can characterize DWDs as detached by eclipses in their light curve or semi-detached (AM CVn) by accretion features and He lines in their spectra (Nissanke et al. 2012). The merger of DWDs may be progenitors to rare massive white dwarfs, solo neutron stars, subdwarf-O stars, or R Corona Borealis stars (Nissanke et al. 2012). DWDs in a subhour binary can also help us study tides, white dwarf internal characteristics, and white dwarf viscosity (Korol et al. 2017).

Another type of UCB is the low-mass X-ray binary (LMXB). X-ray binaries in general are comprised of a massive stellar remnant, either a neutron star or stellar mass black hole, and a companion star, which is usually a main sequence star. The compact object accretes material from the companion star, creating a signature in the X-ray regime. These systems are useful for studying the evolution of massive stars in a binary system and to constrain the physics of core collapse (Type Ibc and Type II) supernovae (Casares et al. 2017). X-ray binaries with a $\leq 1 M_{\odot}$ Roche-lobe filling companion star are further classified as LMXB. The objects in LMXBs corotate in circular orbits (Casares et al. 2017) with short periods on the order of hours. While some systems are eclipsing, non-eclipsing LMXB can also be analyzed if they feature ellipsoidal modulation. As it interacts with its compact companion via Roche lobe, the main sequence star becomes distorted, which causes the projected area of the star to vary as it orbits. This produces a characteristic double-humped, sinusoidal light curve (Charles & Coe 2003).

Verification binaries are located in our own Milky Way Galaxy, therefore, their surface density in the sky should peak near the Galactic Plane. LMXBs in particular are typically located in the Galactic bulge and in globular clusters (Casares et al. 2017). The current sample as in Kupfer et al. (2018) shows sources mostly in the Northern hemisphere at high Galactic latitudes, suggesting the sample is incomplete. Optical surveys such as those utilizing the Zwicky Transient Facility (ZTF) (Graham et al. 2019) and Large Synoptic Survey Telescope (LSST) (Ivezić et al. 2019) should discover more sources to compile a more complete sample of verification binaries. However, many of the degenerate LISA UCBs are inherently faint (up to 70th mag; Korol et al. (2017)) and therefore have not been identified in the EM regime. Half of LMXBs are found within 20 degrees of the center of the galaxy, which makes these systems significantly obscured in the optical regime (Charles & Coe 2003). As for detached DWDs, only 10s of objects have been detected thus far. However, recent literature predicts a number of UCBs that are bright enough to

¹ https://github.com/eXtremeGravityInstitute/LISA_Sensitivity

be detectable in the optical, including 143 short period semi detached binary systems with orbital periods less than 25 min (Nelemans et al. 2004), and 200 detached double white dwarfs (Korol et al. 2017), half of which are eclipsing binaries and half of which are non-eclipsing binaries.

Not every varying light curve, however, will correspond to an eclipsing binary source. The sample will be contaminated with pulsating white dwarfs, Delta Scuti variables, SX Phoenicis stars, and cool spots on the stellar surfaces coming in and out of view as the star rotates (Korol et al. 2017). Analysis of the shape of the light curve as well as the object’s location on an HR diagram will allow us to identify these non-binary, or non-eclipsing binary sources.

Observing UCBs and measuring binary parameters such as radial velocities, masses, and GW strain, will allow us to test binary evolution models, characterize the astrophysical processes occurring in the systems, and contribute to the sample of verification binaries in preparation for the future launch of LISA.

2. METHODS

2.1. Observations

As detailed in Burdge et al. (2019), we have used a Conditional Entropy algorithm (Graham et al. 2013) to period search millions of light curves taken with ZTF, a wide-field (48 square degree) optical survey that scans the Northern sky once every 3 days (Bellm et al. 2019). Next, we visually scanned the light curves for potential UCBs. For sources that fell on the white dwarf region of the HR diagram, based on Gaia colors and magnitudes, I searched for light curves with subhour periods that appeared to be eclipsing. For potential LMXBs, I searched main sequence targets for sinusoidal light curves with a few hour long periods and differential minima. I then cross matched candidates to catalogs such as the Roentgen Satellite (ROSAT) X-ray archive (Voges et al. 1998), and selected new and interesting to follow up on with additional observations.

For DWD candidates, we construct high cadence light curves using the Kitt Peak’s Electron Multiplying CCD (KPED) (Coughlin et al. 2019). For each target, we observe the source for a few hours and make a movie of the source by taking high cadence data with 10 second frames. After confirming the periodicity of the system, these light curves can be modeled using the `e11c` package (Maxted 2016) to create light curve models to fit to the data. These fits will allow us to measure properties of the binary objects such as the relative radii, inclination, and mass ratio. Furthermore, with precise timing and multiple observations over time, we can mea-

sure eclipse timing variations to estimate orbital decay, or \dot{P} . Figure 2 shows an `e11c` generated light curve for an example UCB.

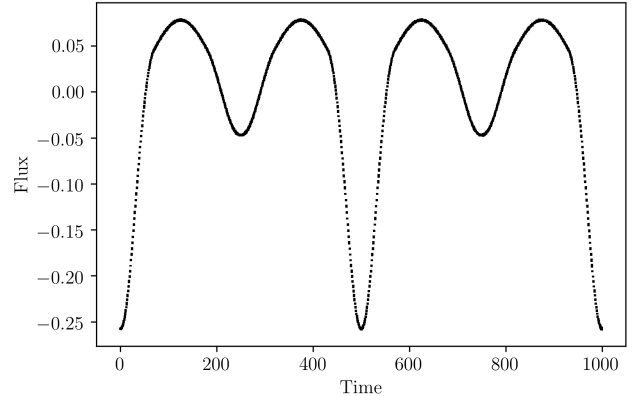


Figure 2. Example of an `e11c` generated light curve for an eclipsing binary system with masses $m_1 = 0.5M_\odot$ and $m_2 = 0.25M_\odot$, relative radii to the semi-major axis $r_1 = R_1/a = 0.5$ and $r_2 = R_2/a = 0.25$, inclination $i = 75^\circ$, and period $P = 500$ s.

We follow up potential LMXBs with phase-resolved spectroscopy to confirm the radial velocities of the system. High radial velocities suggest the main sequence star is in a binary with a compact object such as a black hole or neutron star and is in a LMXB, rather than in a binary with another main sequence star. Furthermore, we can measure properties of the individual objects and the system. By fitting the spectra just after the primary eclipse to stellar models, we can isolate the primary object’s spectrum and measure properties including effective temperature and surface gravity. Spectroscopic data can also reveal details about the system such as the presence of mass transfer or accretion, as detailed in Figure 3 from Burdge et al. (2019).

2.2. Simulations

According to general relativity, the orbital evolution of UCBs with characteristically short periods is primarily driven by GW radiation (Nelemans & van Haaften 2013). This orbital decay manifests in a decreasing period over time, given by

$$\dot{P} = -\frac{96\pi}{5c^5}(G\pi M_c f_{gw})^{\frac{5}{3}} \quad (1)$$

where M_c is the chirp mass ($M_c = (\mu^3 M_{total}^2)^{\frac{1}{5}}$) and f_{gw} is the gravitational-wave frequency ($f_{gw} = \frac{2}{P_{orb}}$).

To simulate light curves with orbital decay, I used the `e11c` package (Maxted 2016) to create eclipsing binary light curves with a constantly changing period. I wrote

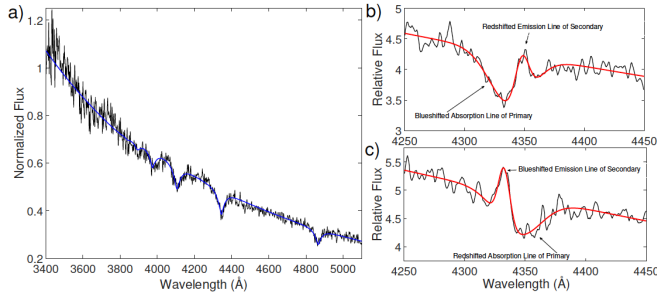


Figure 3. Spectroscopy of ZTF J153932.16+502738.8 from Burdge et al. (2019) taken with LRIS. a) shows the spectrum immediately after the primary eclipse, which isolates the primary object, and the best fitting stellar model (blue line). b) and c) show phase resolved spectra of the hydrogen $n = 5$ to $n = 2$ transition at 4340 Å, which lies within the DBSP wavelength range.

a python script that generates a light curve for a new period at each observation time given by

$$P_{new}(t) = P_0 + \dot{P} * t \quad (2)$$

where P_0 is the starting period and \dot{P} is the rate of orbital decay in units of time/time. General relativity predicts that a typical DWD system with $M_c \sim 0.5 M_\odot$ and a subhour period will have a $\dot{P} \sim -10^{11}$ s/s. To construct a single output light curve from a series of light curves with decreasing periods, I computed the modulated time for each observation time and corresponding P_{new} , and interpolated the individual light curves at the modulus time for each P_{new} . This process returns a single light curve for a given set of binary parameters (including but not limited to mass ratio, inclination, and period) and a rate of orbital decay.

To simulate realistic time sampling, I generated time arrays of length n with Δt between each consequent observation point sampled by a random Gaussian distribution with mean Δt set appropriately according to which survey is being simulated. For ZTF, we expect a 1 year baseline with approximately 3 days between each observation (Bellm et al. 2019), so time sampling parameters were set to $n = 100$ and $\Delta t = 3$. To simulate LSST data, we expect a 10 year baseline with a larger Δt of around 1 week (Ivezić et al. 2019), so time sampling parameters were set to $n = 500$ and $\Delta t = 7$.

Together with a group of researchers at Northwestern University working on LISA science, we are using simulations to constrain the range of DWD systems we will be able to observe with current and upcoming long baseline time domain surveys using ZTF and the Large Synoptic Survey Telescope (LSST) (Ivezić et al. 2019). Our collaborators are putting together a simulated wave-

form catalog of WD binaries using the COSMIC package (Breivik 2018). COSMIC is a package that quickly synthesizes realistic Milky Way compact binary populations. From this binary population catalog, which will target the white dwarf binary population in the Milky Way, we can use the \dot{P} light curve simulating script to generate light curves corresponding to the DWD waveforms.

3. RESULTS

Informed by general relativity, I wrote a script to model light curves of eclipsing binary sources with orbital decay rates calculated from input binary parameters. The program includes modifiable time sampling to simulate realistic observations by wide field surveys such as ZTF and LSST, and will help determine the range of UCBs we can detect with these observations.

On the observational side, I used ZTF scanning to select a sample of UCB candidates to follow up on. From this smaller set of targets, I took spectra of two potential LMXBs, and high cadence photometry of a few potential eclipsing DWDs.

3.1. Observations

I conducted visual scans of ZTF light curves to search for potential UCBs based on criteria informed by the astrophysics of DWDs and LMXBs. After identifying a sample of interesting light curves, I cross checked the coordinates of the objects in SIMBAD to eliminate known sources. A number of known systems were eclipsing contact binaries, which are stars in such a close binary that the stars are touching or partially merged. A few sources were classified as AM Her type stars² (see Figure 4). While these systems are interesting in their own right, as they are already identified, I eliminated them from my search to narrow down the pool of unknown sources which could be verification binaries. In total, I collected 10 LMXB candidate light curves, one of which is shown in Figure 5.

On August 13th, 2019, using Palomar Observatory’s Triple Spectrograph (TSpec) on the 200-inch Hale Telescope, I took 2 hours of near infrared, medium resolution spectroscopy of 2 of the most promising LMXB candidates I had previously identified. Table 1 lists the targets I observed. For ZTFJ16327023, I took a single 300 second exposure, and for ZTFJ18136945, I took two 300

² AM Her type stars are cataclysmic variables—a white dwarf and red dwarf in a close binary—where the white dwarf has a strong magnetic field, and although it has no accretion disk, features an extra long mass transfer stream or accretion column directed along the magnetic field lines straight onto the magnetic poles of the white dwarf.

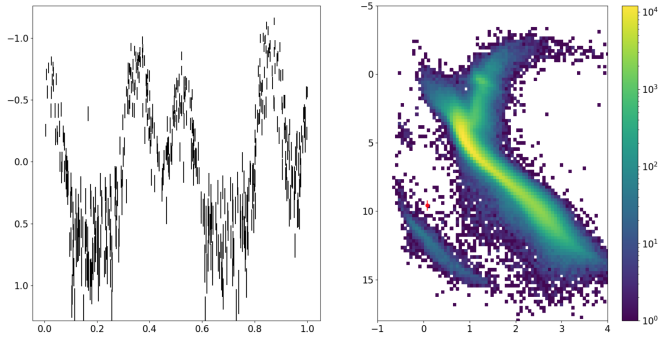


Figure 4. Phase folded ZTF light curve of V* EK UMa, a cataclysmic variable star of AM Her type.

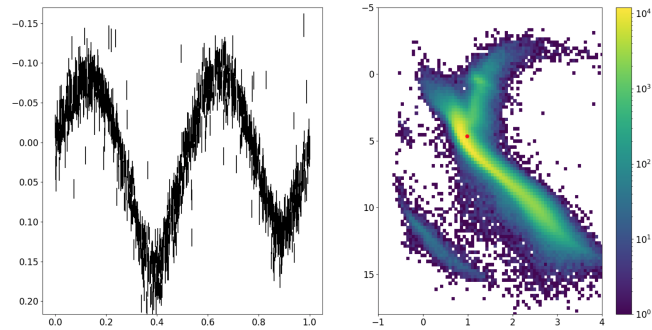


Figure 5. Phase folded ZTF light curve and HR diagram for ZTFJ1813694. With main sequence classification and differential minima without clear differential maxima, it may be a LMXB.

second exposures separated by about 45 min, to collect spectra for multiple phases of the orbit.

Figure 6 shows the reduced spectra of ZTFJ18136945, a candidate LMXB with an expected period of 3.755 hours. Trace 1 is the first exposure, and trace 2 is the exposure taken ~ 45 minutes later. A LMXB with a few hour long period should have a very high radial velocity, which would cause the two traces to be Doppler shifted from each other. As the phase resolved spectra are not shifted, the source is likely not a LMXB.

Object	RA	Dec	Mag	Period (hr)
ZTFJ16327023	248.1941	70.3933	15.157	3.506
ZTFJ18136945	273.4655	69.7561	14.369	3.755

Table 1. Objects observed with TSpec. Each is a potential LMXB with a period on the order of a few hours.

I also used KPED remotely to take high cadence photometric data of a few of the UCB candidates we have identified from the ZTF search (see Table 2). I took an hour or two of data in video mode with 10 second

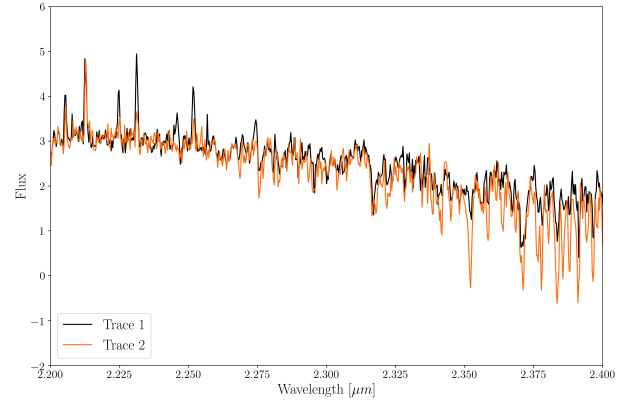


Figure 6. Reduced spectra of ZTFJ18136945, a potential ~ 4 hour period LMXB, with flux plotted in arbitrary units. Trace 1 is the first exposure, and trace 2 is the exposure taken ~ 45 minutes later. As the two traces do not appear Doppler shifted from each other, the target is likely not a LMXB.

frames and 2 by 2 binning for each source. Next, we phase folded by the estimated period from the Conditional Entropy period search algorithm ran on ZTF photometry to confirm the periodicity. Figure 7 shows an example of a recent differential photometric observation of a periodic source. For this target, we confirmed the period of its variability, although it does not appear to be an eclipsing binary source. Another source, ZTFJ18553230, was found to have a much higher period than the period search algorithm detected (103 minutes), as its phase folded light curve did not match this periodicity. This may be due to systematic errors in the period search algorithm from harmonics or photometric calibration.

Object	RA	Dec	Estimated Period (min)
ZTFJ19385841	294.69304	58.69826	27.95 (confirmed)
ZTFJ19260034	291.70128	-0.56820	4.97 (confirmed)
ZTFJ18553230	283.87423	32.50490	103.0

Table 2. Objects observed this summer with KPED. Each is a varying source with a short period, and is a candidate eclipsing DWD. The periods are estimated from the Conditional Entropy period search algorithm ran on ZTF light curves.

3.2. Simulations

With the \dot{P} light curve simulating script, I have generated UCB light curves with orbital decay for ZTF-like and LSST-like time sampling, at a survey time of 1 year and 10 years, respectively. Figures 8 and 9 illustrate the script output for a binary system with properties com-

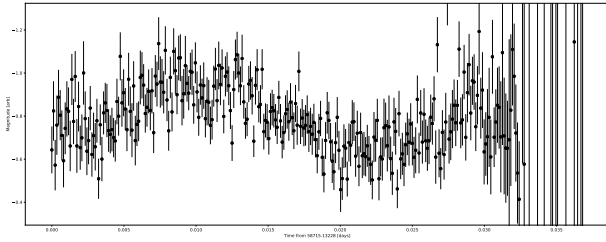


Figure 7. Light curve (plotted in arbitrary magnitude units) for a UCB candidate, ZTFJ19385841, that we observed remotely with KPED. The target shows periodicity at the rate we expect, with a period of 27.95 minutes.

parable to the DWDs studied in [Hermes et al. \(2012\)](#) and [Burdge et al. \(2019\)](#) for each survey. I set a much greater \dot{P} than is astrophysically plausible for better visibility, at $\dot{P} = -1 \times 10^{-7}$. In this example, deviation from mid eclipse point for a system with no orbital decay is clearly detectable for the LSST-like observations, and detectable for the ZTF-like observations.

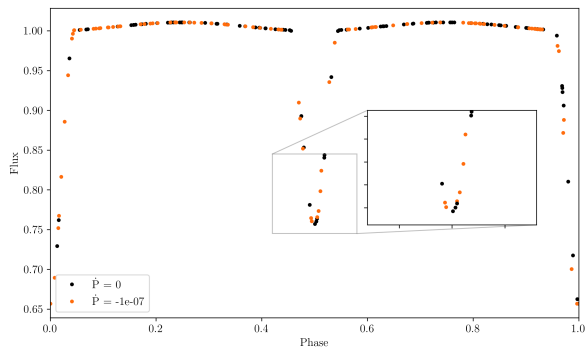


Figure 8. Simulated ZTF phase folded light curve for an eclipsing system with exaggerated orbital decay. The orange points correspond to the case where $\dot{P} = 0$, and the black points simulate a system for which $\dot{P} = -1 \times 10^{-7}$.

4. DISCUSSION

Among the statistical sources of error observationally are read noise from the instruments and Poisson noise from the flux measurements. The data were deliberately taken to be Poisson noise dominated, allowing us to disregard the read noise, as it was negligible in comparison. However, both the spectra and photometry were taken while the moon was near fully illuminated. As the spectra are in the near infrared regime, the moonlight has less of an effect on the data. The photometry was affected by the full moon, though, and limited the quality and depth of our images and increased the photometric error.

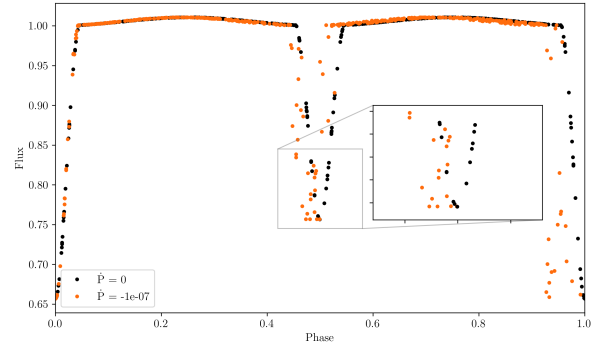


Figure 9. Simulated LSST phase folded light curve for an eclipsing system with exaggerated orbital decay. The orange points correspond to the case where $\dot{P} = 0$, and the black points simulate a system for which $\dot{P} = -1 \times 10^{-7}$.

There are some systematic errors in the period search process, as the Conditional Entropy algorithm assumes the target is periodic. In wide-field, low cadence surveys like ZTF, sometimes the photometric calibration causes objects to appear periodic on time scales that they're not. Due to fluctuations within photometric errors, the search algorithm can sometimes find periodicity where there is no astrophysical variability. Additionally, period searching is sensitive to harmonics, and may find the period to be an integer multiple of the true period if the algorithm identifies a higher or lower order mode of variation. To rule out period search errors, it is important to observe the object for multiple orbits to collect data for multiple periods.

We introduced a few assumptions into our models when simulating the orbital decay light curves. In Figures 8 and 9, we did not account for any weather losses. Once we know what fraction of nights are lost we can better simulate the time sampling and account for weather loss, when no data is taken. Furthermore, Figures 8 and 9 represent an eclipsing system with a higher orbital decay rate than is astrophysically realistic. For typical white dwarf binaries, we expect $\dot{P} \sim -1 \times 10^{-11}$. This small \dot{P} is challenging to detect directly with only 1 year of observation and typical ZTF cadence, even without weather losses, as seen in Figure 10. To qualitatively estimate the minimum survey duration and cadence to detect $\dot{P} \sim -1 \times 10^{-11}$ for a subhour white dwarf binary, I simulated observations of an eclipsing system with time sampling spanning 1-10 years duration and daily-weekly cadence. The phase folded light curves appear more sensitive to increasing duration rather than cadence. Longer surveys like LSST should more easily discover eclipsing binaries with orbital decay than ZTF, but a more robust future analysis of the effects of vary-

ing time sampling would reveal the best parameters for detecting orbital decay.

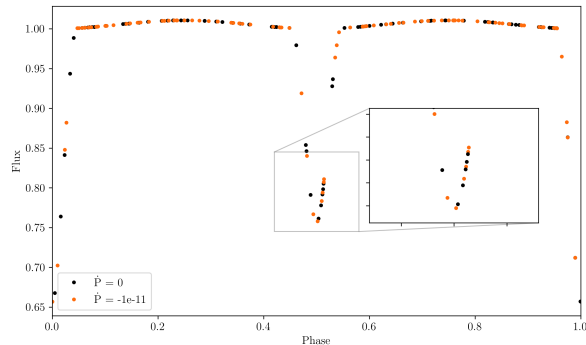


Figure 10. Simulated ZTF-like phase folded light curve for an eclipsing white dwarf binary system with astrophysically realistic orbital decay, $\dot{P} = -1 * 10^{-11}$.

5. CONCLUSION

While the summer resulted in a few observations of potential UCBs, as well as orbital decay models, my work on this project is not done. I plan to continue my work with follow-up observations of UCBs for objects we have already selected, as well as new objects from the most recent ZTF scans.

On the simulation side, along with our collaborators at Northwestern, we are going to use the \dot{P} light curve script and Galactic binary population simulation to quantify the DWDs we expect to be able to observe.

In the more proximate future, I plan to generate simulated \dot{P} light curves spanning inclination and period space and using our period finding script to get a sense for the approximate inclination and period range we are able to measure, down to a minimum significance value of $\sim 7-8$.

The current sample of LISA binaries is incomplete; optical surveys such as ZTF and LSST should discover more sources to compile a more complete sample of verification binaries. Observing UCBs and measuring binary parameters such as radial velocities, masses, and GW strain will allow us to test binary evolution models, characterize the astrophysical processes occurring in the systems, and contribute to the sample of verification binaries in preparation for the future launch of LISA.

Multi-messenger astrophysics provides a new look at the Universe, allowing us to use EM observations to further constrain parameters about the properties of compact binaries observed with GW detectors. Using instruments including ZTF, KPED, and TSpec, we observed these GW sources using photometry and spectroscopy to better understand the astrophysics behind these multi-messenger events.

ACKNOWLEDGEMENTS

Thank you to the LIGO Scientific Collaboration, LIGO Laboratory at Caltech, NSF, and Caltech Student-Faculty Programs for supporting this work. In particular, I would like to acknowledge my mentors, Michael Coughlin and Shreya Anand, as well as Michael Katz, Alan Weinstein, Kevin Burdge, Kishalay De, and my fellow undergraduate researchers for their advice, mentorship, and camaraderie.

REFERENCES

- Bellm, E. C., Kulkarni, S. R., Graham, M. J., et al. 2019, *PASP*, 131, 018002, doi: [10.1088/1538-3873/aaecbe](https://doi.org/10.1088/1538-3873/aaecbe)
- Breivik, K. 2018, PhD thesis, Northwestern University
- Burdge, K. B., Coughlin, M. W., Fuller, J., et al. 2019, *Nature*, 571, 528, doi: [10.1038/s41586-019-1403-0](https://doi.org/10.1038/s41586-019-1403-0).
- Casares, J., Jonker, P. G., & Israelian, G. 2017, *X-Ray Binaries*, 1499, doi: [10.1007/978-3-319-21846-5_111](https://doi.org/10.1007/978-3-319-21846-5_111)
- Charles, P. A., & Coe, M. J. 2003, arXiv e-prints, astro. <https://arxiv.org/abs/astro-ph/0308020>
- Coughlin, M. W., Dietrich, T., Doctor, Z., et al. 2018, *MNRAS*, 480, 3871, doi: [10.1093/mnras/sty2174](https://doi.org/10.1093/mnras/sty2174)
- Coughlin, M. W., Dekany, R. G., Duev, D. A., et al. 2019, *MNRAS*, 485, 1412, doi: [10.1093/mnras/stz497](https://doi.org/10.1093/mnras/stz497)
- Graham, M. J., Drake, A. J., Djorgovski, S. G., Mahabal, A. A., & Donalek, C. 2013, *MNRAS*, 434, 2629, doi: [10.1093/mnras/stt1206](https://doi.org/10.1093/mnras/stt1206)
- Graham, M. J., Kulkarni, S. R., Bellm, E. C., et al. 2019, *PASP*, 131, 078001, doi: [10.1088/1538-3873/ab006c](https://doi.org/10.1088/1538-3873/ab006c)
- Hermes, J. J., Kilic, M., Brown, W. R., et al. 2012, *ApJL*, 757, L21, doi: [10.1088/2041-8205/757/2/L21](https://doi.org/10.1088/2041-8205/757/2/L21)
- Hotokezaka, K., Nakar, E., Gottlieb, O., et al. 2018, arXiv e-prints, arXiv:1806.10596. <https://arxiv.org/abs/1806.10596>
- Ivezić, Ž., Kahn, S. M., Tyson, J. A., et al. 2019, *ApJ*, 873, 111, doi: [10.3847/1538-4357/ab042c](https://doi.org/10.3847/1538-4357/ab042c)
- Korol, V., Rossi, E. M., Groot, P. J., et al. 2017, *MNRAS*, 470, 1894, doi: [10.1093/mnras/stx1285](https://doi.org/10.1093/mnras/stx1285)

- Kupfer, T., Korol, V., Shah, S., et al. 2018, MNRAS, 480, 302, doi: [10.1093/mnras/sty1545](https://doi.org/10.1093/mnras/sty1545)
- LISA Scientific Collaboration. 2017, arXiv e-prints, arXiv:1702.00786. <https://arxiv.org/abs/1702.00786>
- Maxted, P. F. L. 2016, ellc: Light curve model for eclipsing binary stars and transiting exoplanets. <http://ascl.net/1603.016>
- Nelemans, G., & van Haften, L. 2013, in *Astronomical Society of the Pacific Conference Series*, Vol. 470, 370 *Years of Astronomy in Utrecht*, ed. G. Pugliese, A. de Koter, & M. Wijburg, 153. <https://arxiv.org/abs/1302.0878>
- Nelemans, G., Yungelson, L. R., & Portegies Zwart, S. F. 2004, MNRAS, 349, 181, doi: [10.1111/j.1365-2966.2004.07479.x](https://doi.org/10.1111/j.1365-2966.2004.07479.x)
- Nissanke, S., Vallisneri, M., Nelemans, G., & Prince, T. A. 2012, ApJ, 758, 131, doi: [10.1088/0004-637X/758/2/131](https://doi.org/10.1088/0004-637X/758/2/131)
- Robson, T., Cornish, N. J., & Liug, C. 2019, *Classical and Quantum Gravity*, 36, 105011, doi: [10.1088/1361-6382/ab1101](https://doi.org/10.1088/1361-6382/ab1101)
- Rosswog, S., Sollerman, J., Feindt, U., et al. 2018, A&A, 615, A132, doi: [10.1051/0004-6361/201732117](https://doi.org/10.1051/0004-6361/201732117)
- Voges, W., Boller, T., Dennerl, K., et al. 1998, in *Science with XMM*, 38